Ultra-Low Power Solar Energy Harvester for IoT Edge Node Devices

Saswat Kumar Ram, *Student Member, IEEE*, Banee Bandana Das, *Student Member, IEEE*, Ayas Kanta Swain, *Member, IEEE*, Kamalakanta Mahapatra, *Member, IEEE*

***Abstract*—An Ultra-low power solar energy harvesting system (EHS) for IoT end node devices is presented in this paper. To provide an uninterrupted power supply to IoT nodes is a challenge. The solar cell is used as an input source and this low input voltage is boosted by using the DC-DC converter. The charge pump is used as a voltage booster and the impedance matching between the solar cell and the converter is achieved through frequency tuning and capacitor value modulation. A hill-climbing technique is used for maximum power point (MPP) achievement. The EHS designed is self-sustainable and the output is in the range of 3-3.55 V with an input of 1-1.5 V. The EHS is designed in CMOS 90 nm technology library. The simulation results validate the proposed concept and the EHS is consuming a power of 22 μW, which is within the Ultra-low power range of IoT smart nodes.**

***Index Terms*—Charge Pumps, Internet of Things (IoT), Wireless Sensor Networks (WSNs), Capacitor Value Modulation (CVM), Resistor Bank.**

I. Introduction

RApid growth in IC fabrication leads to autonomous controlling of consumer electronics products [1], [2], wireless sensor networks [3] and in implantable bio-medical applications [4]. The bottle neck of these applications is in the power supply. An uninterrupted power supply is needed for a continuous operation without much maintenance [5]. A promising technique to mitigate this is by harnessing the available natural energy resources [6], [7]. The solar [8], [9], piezoelectric, wind, microbial etc., can be chosen as an alternative to increase the lifetime of the rechargeable batteries. The storage of the energy is of most important as the multiple loads demands different levels of power. The storage in super-capacitor [10] lasts for minimum ten years without any maintenance [8], [11]. The switched capacitor boost converter is also called as charge pumps [8] are preferred than the inductor based boost converters for on-chip implementation. In [11], [12] researchers discussed harvesting system design with maximum power tracking [13]. The control section monitors the harvesting system operation using finite state machines (FSM) [14], [15]. The summary of the related work is presented in Table I, which includes methodology used with a brief discussion. The most decisive parameter for a DC-DC converter [11] is its efficiency and is described as follows.

$$\eta = \frac{P_{out}}{P_{in}} \times 100\% = \frac{P_{out}}{P_{out} + P_{loss}} \times 100\% \qquad (1)$$

The power loss (P_{loss}) includes the switching loss, redistribution loss and conduction loss due to which the efficiency is less than 100%.

In this paper section I is the introduction. Section II is the proposed energy harvesting system. section III presents the experimental setup and section IV is the conclusion.

The discussion on energy harvesting sources indicates the solar energy as a compatible energy source due to its wide availability and attainment of direct DC from it. The varying load conditions needs a constant supply voltage and the varying input source makes the system complex. A variable frequency for DC-DC converter can tackle the variable load [16] and the varying input source. The CVM is also used for achieving the MPPT. A hill-climbing MPPT technique is adopted for impedance matching between the solar and the DC-DC converter. The contribution of this paper is as follows:

- A novel two dimensional tuning of for impedance matching of the converter and solar cell.
- A novel ultra-low power self-sustainable solar energy harvesting system (PV-EHS) design.

II. Proposed Energy Harvesting System

Fig. 1 shows the block diagram of the energy harvesting system (EHS). The EHS comprises of (a) digital supply control oscillator (b) non-overlapping clock generator with level shifter (c) Auxillary charge pump (d) DC-DC converter (e) Current sensor (f) FSM controller with MPPT module.

A. Digital Supply Controlled Oscillator (DCO)

Fig. 2 shows the digital supply control oscillator. The control action of the oscillator is depending on the supply, which is controlled by a low drop-out regulator (LDO). A resistance R_1 is controlling the output voltage of LDO. The R_1 is a resistance switch box as shown in the Fig. 3. The resistance box is a stack of resistances of equal value. Each resistance has a parallel PMOS switch, which can be ON or OFF using control thermometer bits (b_0- b_{15}). When the PMOS is OFF a resistance is included to the stack and supply voltage increases. As the supply voltage increases the frequency also get increased. With increase in frequency the converter output also get boosted with improved efficiency.

B. Non-overlapping clock generator (NOCG) with level shifter and auxiliary Charge Pump (ACP)

The DCO generates the essential clock frequency and is given to NOCG. The NOCG generates two non-overlapping clocks for the ACP and the level shifter (LS) with reduced shoot through effect. The LS and ACP provides the switching

TABLE I
SUMMARY OF RELATED WORK

Sl.No.	Reference	Methodology	Discussion
1	[7]	Dynamic Input Impedance Matching	⇒ Multi array TEG as input energy source for harvesting. ⇒ MPPT technique for boost converter. ⇒ Control module is complex.
2	[11]	Re-configurable Charge Pump with two Dimensional MPPT	⇒ Design of reconfigurable charge pump for achieving different CGs. ⇒ Frequency modulation scheme for MPPT procedure. ⇒ Constant on time scheme used for load regulation. ⇒ Circuit topology is complex.
3	[13]	Hybrid MPPT Controller	⇒ Serial switch for doubling the input voltage. ⇒ Compact size analog MPPT controller design.. ⇒ Detection of power slope characteristics of solar cell.
4	[12]	Adaptive MPPT for Harvesting System	⇒ Inductor less design with regulated charge pump. ⇒ Optimum power point algorithm (OPPT) for MPPT for Indoor light conditions. ⇒ Application limited to indoor lightning.

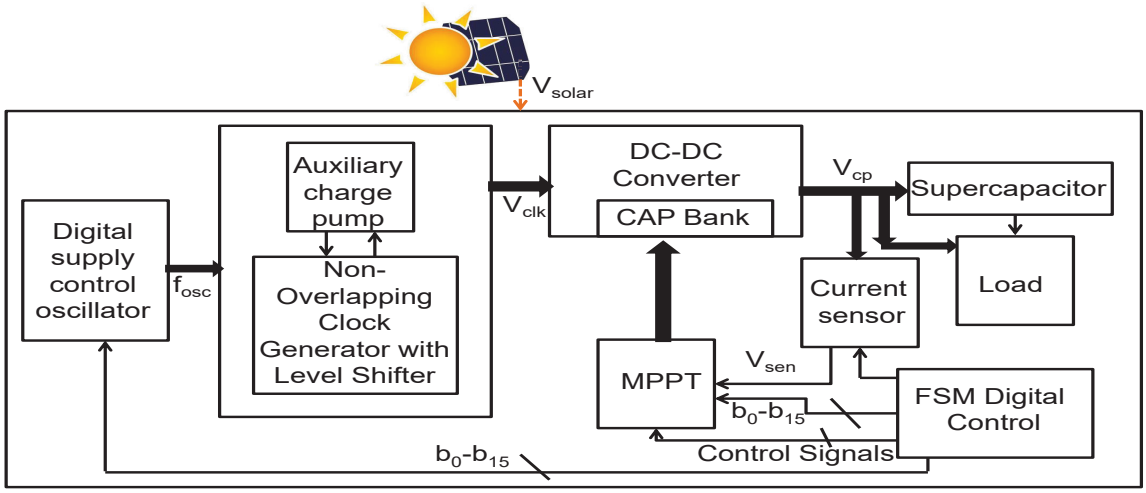

Fig. 1. Block Diagram of Proposed reliable and secure Energy Harvesting System

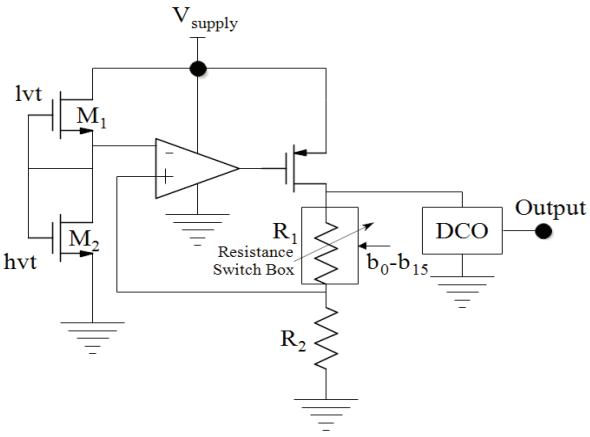

Fig. 2. Digital Supply Control Oscillator

signals and other biases for DC-DC converter. The LS is used to boost the clock amplitude for reducing the losses due to charge transfer during voltage boosting.

C. Charge Pump as Voltage Tripler

Fig. 4 depicts the charge pump (CP) as a voltage tripler, which is the combination of voltage doublers. The boosting of

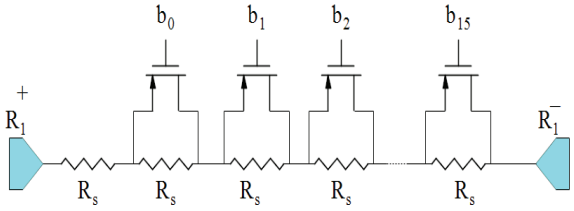

Fig. 3. Programmable Resister Bank

voltages in the converter is achieved by applying alternative clock pulses to charge the solar energy across the capacitors C_u, which includes power capacitors C_1, C_2, C_3, C_4 and level up the negative plate by the same potential. The harvesting system designed is for IoT nodes having sensor devices that needs 3.3V supply. The cross-coupled MOSFETs MN_1 and MN_2 in Fig. 4 are driven separately by high voltages; such that low turn-on voltage can be overcome thereby reducing the conduction resistance. The impedance of the voltage tripler is given by [11]

$$Z_{cp} = \frac{V_{solar}}{I_{in}} = \frac{1}{2f_s C_u} \frac{1+\alpha}{\left(3 - \frac{V_{out}}{V_{solar}}\right)\alpha} \tag{2}$$

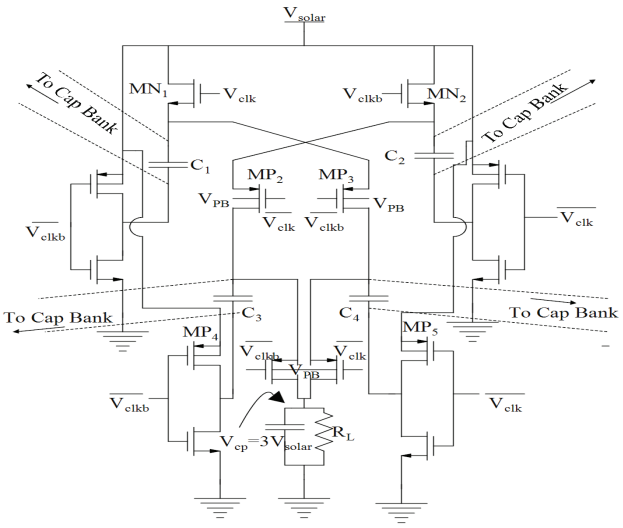

Fig. 4. Circuit diagram of Charge Pump as a Voltage Tripler

Equation 2 indicates that the impedance of the charge pump is inversely proportional to C_u. α is the capacitor ratio between the first and second stage. The capacitor C_u is connected to programmable capacitor banks for impedance matching through CVM [8]. From the small signal model of a tripler [11], it can be observed as Equation 3.

$$[2V_{solar} - (V_{out} - V_{solar})] \times \alpha C_u = \frac{1}{2} \times \frac{T \times V_{out}}{R_L} \quad (3)$$

where T and R_L are the switching period and load of the SoC respectively. By rearranging equation 3 it can be written as

$$V_{solar} = \left(\frac{1}{2} * \frac{T}{R_L} * \frac{1}{\alpha C_u} + 1\right) * \frac{1}{3} * V_{out} \underrightarrow{Match} V_{MPP} \quad (4)$$

From Equation 4, it is found that, the MPP is achieved by varying the frequency f and capacitor C_u. The frequency is varied using DCO and a variable C_u is used for impedance matching. The power capacitors are digitalized as capacitor banks; as digital implementation consumes less power with reduced noise. The power conversion efficiency (PCE) is a measure of boosting of input as per conversion ratio and is given by Equation 5.

$$PCE = \frac{V_{out}}{V_{solar} \times CR} \times 100\% \quad (5)$$

The output of the converter is sensed through a current sensor and hill-climbing MPPT is used for MPP achievement [8]. A dedicated FSM [8] controller is used for controlling the entire operation.

III. SIMULATION RESULTS

The solar energy harvesting system (PV-EHS) is designed in CMOS 90nm technology library. The capacitors used in the converter and capacitor banks are MIM (Metal-Insulator-Metal) capacitors. The digital capacitor bank is used for impedance matching through CVM. The V_{solar} is in the range of 1-1.5V (with temperature 27°C). The load was designated with a resistor in range 200KΩ to 10MΩ in parallel with a super-capacitor having 33mF value.

The simulation result shows that with variation in supply voltage of the DCO, leads to generation of different frequencies for frequency tuning during the MPPT process and is depicted in Fig. 5.

The variable frequency generated by the DCO using the LDO leads to better boosted output of the converter and is shown in the Fig. 6. The voltage conversion efficiency of the converter is improved using the frequency generated by the DCO. Fig. 7 depicts the complete simulation results of the

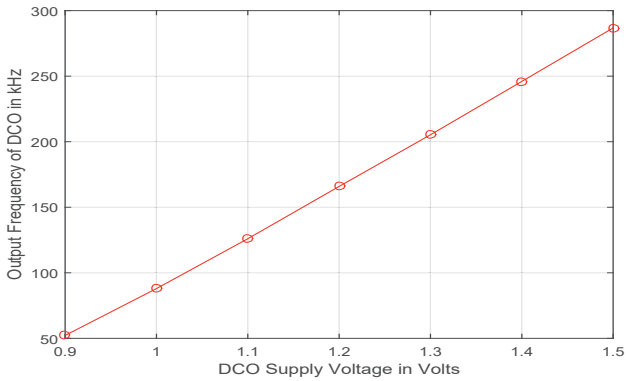

Fig. 5. Variation of DCO output with Supply Voltage

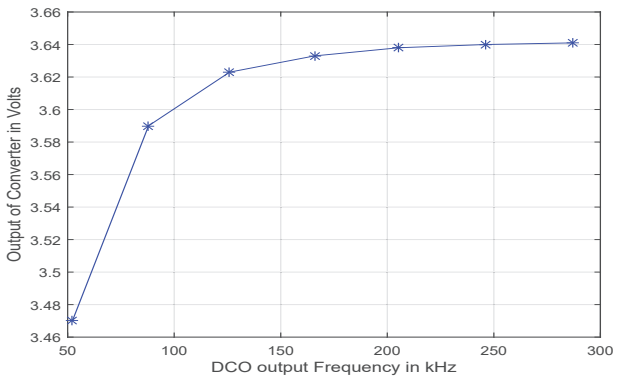

Fig. 6. Variation of Converter output with Frequency

EHS with MPPT. The V_{solar} is the solar voltage and is used for the total EHS as a supply. The RSC_{clk} is the clock generated from the DCO. As per the thermometer codes generated by the FSM for MPPT the resister bank is selected at LDO for frequency tuning. The tuning of frequency can be seen in the clock output. The higher bias (out) for the level shifter and converter is generated by the auxiliary charge pump (out=3V). The boosted output of the converter (V_{out}) is in the range of 3-3.5V and is used to charge the super-capacitor and tackle the load as depicted in Fig. 7.

A current sensor senses the output of the converter (V_{out}) at intervals as V_{sens} and is stored in the sample and hold circuits S/H_1 and S/H_2 (as V_{out1} and V_{out2}) as depicted in Fig. 7. The thermometer codes (b_0-b_{15}) are used for tuning. The control signals (S_{sen}, S_1, S_2, S_3, S_4) involved for the process of MPPT decision is depicted in Fig. 7. The power information

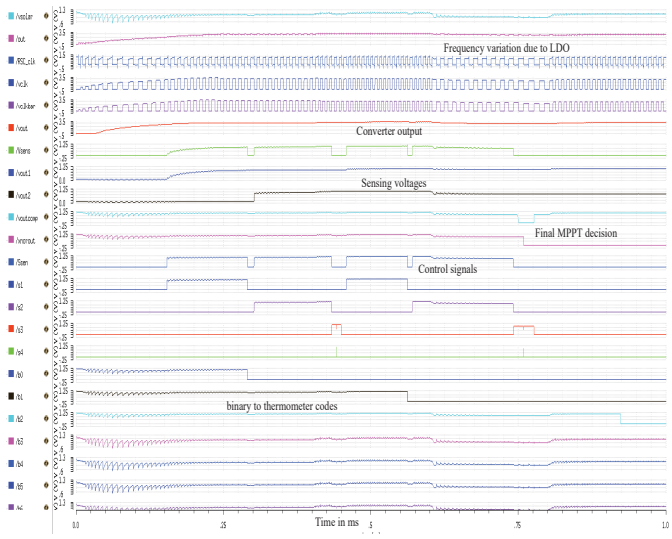

Fig. 7. Simulation result of EHS with MPPT achievment

stored in the sample and hold circuits are compared and MPPT decision is taken as per hill-climbing procedure. Once the old power is more than the new power then the $V_{outcomp}$ becomes Low from High state, the final MPPT decison bit X_{norout} becomes Low from High state. The Low in X_{norout} makes all the control signals to reset as indicated in Fig. 7, thereby charging the super-capacitor and supply to load. A comparative analysis of this work with other state of art EHS is presented in Table II.

IV. Conclusion

The failure of sensor nodes due to power failure in the IoT scenario is a catastrophic situation. The denial of service type attack may cause information loss in IoT. The solar energy harvesting is a well-suited alternative towards green and clean energy. The solar energy harvesting system (PV-EHS) designed for a minimum voltage of 1.22V as MPP in the range of 1-1.5V. The output of the EHS is in between 3 to 3.55 V , which satisfies many IoT end node device supply requirement. The efficiency of the DC-DC converter is in the range of 87% to 97%. The only input is the solar voltage and no external bias is need for any operation. The higher bias voltages needed are generated on-chip. The EHS designed is self-sustainable and consuming power of 22 μW, which is under ultra-low power range.

TABLE II
Comparison of Different Low Energy Harvesting System

Design Parameters	DICM [5]	FOCV [10]	HC [9]	NFC [12]	Proposed
Sensors Required	No	Yes	Yes	No	No
Micro controllers Required	No	Yes	No	No	No
Adaptive MPPT	No	No	Yes	Yes	Yes
Impedance Matching	NA	Duty Ratio	f	f	CVM + RVM
Switching Converter	NA	Inductor	Capacitor	Capacitor	Capacitor
Self-Startup	NA	No	Yes	Yes	Yes
Technology	NA	NA	350 nm	180 nm	90 nm

ACKNOWLEDGEMENT

This research work is supported by Special Manpower Development Program for Chips to System Design (SMDP-C2SD) of Government of India.

References

[1] P. Sundaravadivel, E. Kougianos, S. P. Mohanty, and M. K. Ganapathiraju, "Everything you wanted to know about smart health care: Evaluating the different technologies and components of the Internet of Things for better health," *IEEE Consumer Electronics Magazine*, vol. 7, no. 1, pp. 18–28, 2017.

[2] S. P. Mohanty, U. Choppali, and E. Kougianos, "Everything You wanted to Know about Smart Cities: The Internet of Things is the backbone," *IEEE Consumer Electronics Magazine*, vol. 5, no. 3, pp. 60–70, July 2016.

[3] B. B. Das and S. K. Ram, "Localization using beacon in wireless sensor networks to detect faulty nodes and accuracy improvement through dv-hop algorithm," in *2016 International Conference on Inventive Computation Technologies (ICICT)*, vol. 1. IEEE, 2016, pp. 1–5.

[4] B. B. Das, P. Kumar, D. Kar, S. K. Ram, K. S. Babu, and R. K. Mohapatra, "A spatio-temporal model for eeg-based person identification," *Multimedia Tools and Applications*, pp. 1–21, 2019.

[5] V. Raghunathan, A. Kansal, J. Hsu, J. Friedman, and M. Srivastava, "Design considerations for solar energy harvesting wireless embedded systems," in *Proceedings of the 4th international symposium on Information processing in sensor networks*. IEEE Press, 2005, p. 64.

[6] A. Omairi, Z. H. Ismail, K. A. Danapalasingam, and M. Ibrahim, "Power harvesting in wireless sensor networks and its adaptation with maximum power point tracking: Current technology and future directions," *IEEE Internet of Things Journal*, vol. 4, no. 6, pp. 2104–2115, 2017.

[7] S. Carreon-Bautista, A. Eladawy, A. N. Mohieldin, and E. Sánchez-Sinencio, "Boost converter with dynamic input impedance matching for energy harvesting with multi-array thermoelectric generators," *IEEE Transactions on Industrial Electronics*, vol. 61, no. 10, pp. 5345–5353, 2014.

[8] S. K. Ram, S. R. Sahoo, K. Sudeendra, and K. Mahapatra, "Energy efficient ultra low power solar harvesting system design with mppt for iot edge node devices," in *2018 IEEE International Symposium on Smart Electronic Systems (iSES)(Formerly iNiS)*. IEEE, 2018, pp. 130–133.

[9] H. Shao, C.-Y. Tsui, and W.-H. Ki, "The design of a micro power management system for applications using photovoltaic cells with the maximum output power control," *IEEE Transactions on Very Large Scale Integration (VLSI) Systems*, vol. 17, no. 8, pp. 1138–1142, 2009.

[10] F. Simjee and P. H. Chou, "Everlast: long-life, supercapacitor-operated wireless sensor node," in *Proceedings of the 2006 international symposium on Low power electronics and design*. ACM, 2006, pp. 197–202.

[11] X. Liu, L. Huang, K. Ravichandran, and E. Sánchez-Sinencio, "A highly efficient reconfigurable charge pump energy harvester with wide harvesting range and two-dimensional mppt for internet of things," *IEEE Journal of Solid-State Circuits*, vol. 51, no. 5, pp. 1302–1312, 2016.

[12] S. Mondal and R. Paily, "On-chip photovoltaic power harvesting system with low-overhead adaptive mppt for iot nodes," *IEEE Internet of Things Journal*, vol. 4, no. 5, pp. 1624–1633, 2017.

[13] C.-Y. Yang, C.-Y. Hsieh, F.-K. Feng, and K.-H. Chen, "Highly efficient analog maximum power point tracking (AMPPT) in a photovoltaic system," *IEEE Transactions on Circuits and Systems I: Regular Papers*, vol. 59, no. 7, pp. 1546–1556, 2012.

[14] S. K. Ram, S. R. Prusty, P. K. Barik, K. Mahapatra, and B. Subudhi, "FPGA implementation of digital controller for active power line conditioner using SRF theory," in *Proceedings of the 10th International Conference on Environment and Electrical Engineering*, 2011, pp. 1–5.

[15] S. K. Ram and B. B. Das, "Comparison of different control strategy of conventional and digital controller for active power line conditioner (APLC) for harmonic compensation," in *2013 12th International Conference on Environment and Electrical Engineering*. IEEE, 2013, pp. 209–214.

[16] M. Ibrahim, A. Eltaliawy, H. Mostafa, and Y. Ismail, "A new digital current sensing technique suitable for low power energy harvesting systems," in *5th International Conference on Energy Aware Computing Systems & Applications*. IEEE, 2015, pp. 1–4.